Internal document JGW-T2011582

IP sensor correction and X-arm cavity length change

Additional notes for PhD thesis by Y. Fujii

May 5, 2020

Department of Astronomy, Graduate School of Science,
The University of Tokyo

Yoshinori Fujii

Abstract

1. This document reports the measured performance of the sensor correction system installed to the IP-stage (IPsc). We measure the reduction of the X-arm cavity length change when the IPsc of both ETMX and ITMX suspensions is (and is not) included to the damping control system.

2. Originally this work is motivated to compare this sensor correction performance by the seismometers to that by the geophysical interferometer (GIF) discussed in [1].

3. The measurement campaign has been done in September 2019. In particular, the measurement summarized in this document has been done on September 24th, 2019. The corresponding measurement files are stored in /users/VIS/TypeA/general/rms_suppression/20190924/

4. Other notes can be found in the below (not summarized though): https://github.com/YoshinoriFujii/Weekly-task/issues

5. This document refers thefollowing descriptions:,

   - section 4.2, Active vibration isolation in [2], for the background of the control system used in this document.
   - section 7.3 in [2], for more detailed information about the implemented damping filters filters in this work (especially for ETMX suspension):
   - section 7.4 in [2], for the sensor-correction filters (especially for ETMX suspension).

6. As the result:

   - It is measured that the IP_{sc} at both ETMX and ITMX suspension reduces the RMS displacement of the X-arm cavity length change by a factor of 2 (if the integration is done down to 40 mHz).
   - When the IP_{sc} is *not* engaged, the seismic noise coupling in L degree fo freedom (DoF) can explain the X-arm cavity length change, except for the frequencies around 150 mHz and 400 mHz.
   - When the IP_{sc} is engaged, seismic noise coupling in L DoF cannot explain the X-arm cavity length change. It seems that the other DoFs than L DoF affect the the X-arm cavity length change.

7. In order to suppress the RMS displacement more, the following work seems to work:

    - To reduce the noise coupling of the IX seismometer, in particular below 0.1 Hz. This is so if we want to keep using the sensor correction system.
    - To reduce the coupling from the other DoF than L DoF, for both the ETMX and ITMX suspension. It seems to be the same issue found in [1].
    - To damp the residual 150 mHz mode by closing the damping loop which senses the lower stage motion. For example, BF sensor to BF actuator, TM sensor to IP actuator, TM sensor to BF actuator, or BF sensor to IP actuator. For this purpose, however, we will have some difficulties.
        (a) If we use BF sensor signals, we will not be able to have sufficient open loop gain around 250 mHz due to the mechanical response. Also, we need to use the sensor correction at the BF-stage for this purpose. Thus we will additionally induce the low frequency displacement due to the seismometer tilt-coupling.
        (b) If we use TM sensor signals, we will just induce the noise due to the sensor noise of the length optical lever. We need to reduce the noise level of the current length-oplev first. Then we might have to use the sensor correction at the TM-stage as well.

8. It must be noted that:

    - Some of the plots, such as the coherence and the result of the bruco, are missing in this document. The corresponding data have to be dug out from the Kashiwa-server. That work has not yet done on May 5, 2020.

Table of Contents

Chapter 1

Measurement setup

The setup for this measurement is described. In particular, we focus on about the setting for the X-arm cavity, the ETMX suspension and ITMX suspension.

1.1 X-arm cavity

See section 5.1 in [1]. Same configuration is used in this work as well. The X-arm cavity is locked with the IR laser. During the measurement, to keep the X-arm cavity on resonance, the signals is fed back to the frequency actuator (AOM).

1.2 ETMX suspensions

The measured mechanical responses are summarized in section 7.2 in [2].

It must be noted that the F2-GAS filters is mechanically stuck for a technical reason. Thus the vibration isolation performance above 2 Hz is degraded as summarized in section A.1. However, this degrade does not affect the RMS motion much. Thus we do not investigate this issue here.

1.2.1 Control filters for ETMX

See section 7.3 and 7.4 in [2].

1.2.2 Sensor correction performance of ETMX

See section 7.4.2 in [2].

1.3 ITMX suspensions

The measured mechanical responses will summarized in somewhere. It is confirmed that the mechanical transfer functions of the ITMX suspension are consistent with the ones of the ETMX suspension[1].

It must be noted that the F0-GAS filters is mechanically stuck for a technical reason. Thus the vibration isolation performance above 2 Hz is degraded as summarized in section A.1. However, this degrade does not affect the RMS motion much. Thus we do not investigate this issue here.

1.3.1 Control filters for ITMX

We close the same-shape control filters as ETMX suspension, to the ITMX suspension. We adjust the cut-off frequencies and gains in an ad-hoc way. We then implement the sensor correction filter F_{sc} to the ITMX IP.

Concerning the sensor correction filter for ITMX, we design the same filter as the one used for ETMX suspension. We then adjust the parameters such as the cut-off frequency of the high-pass filter. This is done since the noise coupling at frequencies below 0.1 Hz of the seismometer (Trillium120QA) at the IX station are higher than the one at the EX station.

More concretely, we use an elliptic high-pass filter with 20 mHz cut-off whose order, pass-band ripple and the attenuation are set to second, 10 dB and 80 dB respectively, for the high pass filter.

We also included a high-pass filter at 0.5 mHz with forth order of Butterworth for the compensation of f^{-1} component in the seismometer calibration filter S_s. The total phase shift at 0.1 Hz due to this filter is given by 6.3 deg, which give 0.6 % difference.

1.3.2 Sensor correction performance of ITMX

Figure 1.1 shows the spectra of the IP displacement of ITMX suspension, measured by the TAMA accelerometers ($left$) and by the LVDTs ($right$), when the $\mathrm{IP_{sc}}$ is on and off. The seismometer signals are included to confirm the ground motion can be regarded as the identical between the two measurements.

With the $\mathrm{IP_{sc}}$, the IP-stage motion is suppressed at least by a factor of 3 at 250 mHz according to Figure 1.1 ($left$). However, the IP-stage motion level becomes below the accelerometer noise floor. We then cannot measure the actual suppression performance from this plot.

Figure 1.2 show the comparison between the sensor-corrected IP-LVDT signal and the TAMA accelerometer signal when the IPsc is on. In the frequency region between 0.3 Hz and 1 Hz, both the spectra are consistent.

[1] *Where is the reference? The diaggui data has to exported and summarized.*

However, it is expected that there might be a discrepancy between the accelerometer signal and the sensor-corrected IP-LVDT signal below 0.3 Hz. Similar to the ETMX case (see section 7.4.2 in [2]), we might observe the tilt coupling of the TAMA accelerometer. The details will be investigated in the future.

Figure 1.3 shows the comparison of teh BF-stage displacement spectrum measured by the not-sensor-corrected LVDTs when the IP_{sc} is on and off. Also in this case, most of the BF-stage displacement spectra are below the sensor noise level above 40 mHz. At frequencies between 10 mHz to 40 mHz, the displacement enhancement due to the seismometer coupling is observed as expected.

Concerning the TM-stage signal, the measurement by the length-oplev is not included here since the measured spectra show only the sensor noise even without the IPsc.

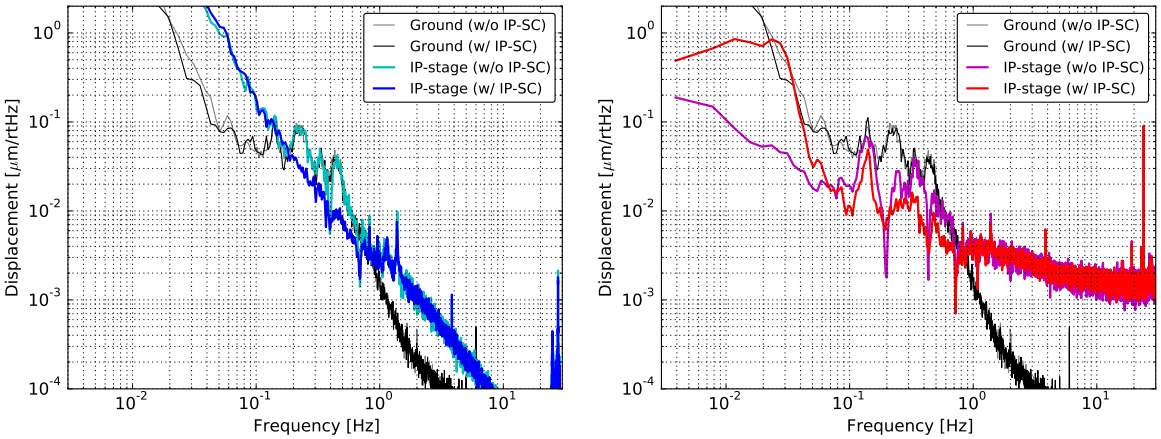

Figure 1.1: Comparison of the IP-stage displacement spectrum measured by the inertial sensor, the TAMA accelerometer (*left*) and by the LVDT (*right*) when the IPsc is on and off at ITMX suspension. I note that in the *left* panel, the LVDT signal with and without IPsc is not compatible since one measures the displacement, while the other one observes the inertial motion basically.

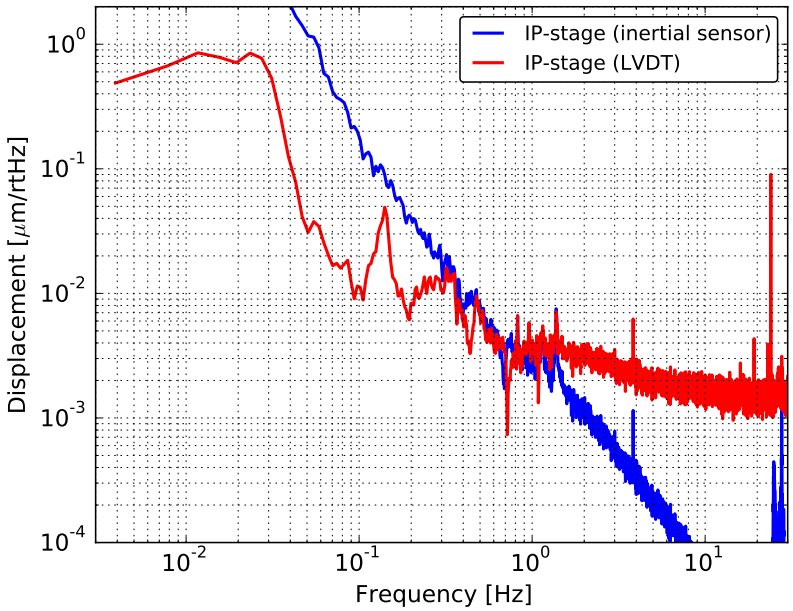

Figure 1.2: Comparison between the sensor-corrected IP-LVDT signal and the TAMA accelerometer signal when the IPsc is on.

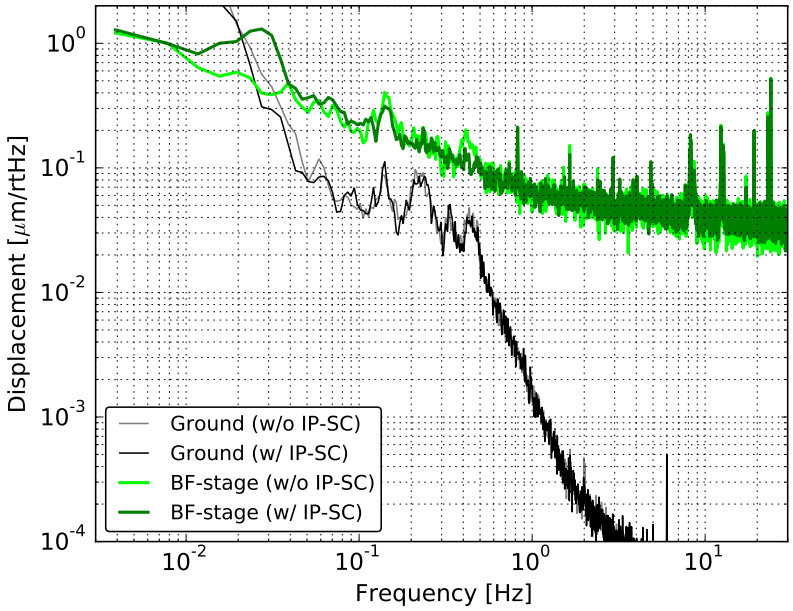

Figure 1.3: Comparison of the BF-stage displacement spectrum measured by the LVDT when the IPsc is on and off at ITMX suspension.

Chapter 2

Measurement with X-arm cavity

We measure how the sensor correction technique suppresses the one arm-cavity length change using the X-arm cavity.

In this measurement, we cannot investigate the detailed sensor correction performance of the ITMX suspension, due to the noise levels of the local sensors. However, we assume that the suppression performance of the ITMX suspension is consistent to the one of the ETMX suspension[1].

2.1 Difference among the X-arm cavity axis and local sensors of X-arm suspensions

We first measure how much the axes are different between the X-arm cavity axis and the local sensor ones of the ETMX and ITMX suspensions. This is a supplementary measurement for the transfer function measurement with the FPMI.

The purpose is to confirm the ETMX and ITMX suspensions are sufficiently aligned to the X-arm cavity axis.

The angle difference is estimated by measuring and comparing the following the two transfer functions at 10 mHz:

1. the transfer function from displacement of the suspension in the Longitudinal DoF to the X-arm cavity length change,

2. the transfer function from displacement of the suspension in the Transverse DoF to the X-arm cavity length change.

These two kinds of transfer functions are measured by actuating the stage at 10 mHz. For example, for the IP-stage case, the angle which describes the axis difference θ is obtained by:

$$\theta \;=\; \arctan\left(\frac{X_{\mathrm{arm}}}{IP_{\mathrm{T}}} \Big/ \frac{X_{\mathrm{arm}}}{IP_{\mathrm{L}}}\right). \tag{2.1}$$

[1] *If necessary, please measure the detailed sensor correction performance of ITMX (and Y-arm suspensions as well) somehow. The first thing would be to check the transfer function from thr ground displacement to the TM displacement as shown in section 7.4 in [2].*

During this measurement, the X-arm cavity is locked with IR laser and the cavity length change signal is reconstructed from its control signal (see section 5.1 in [1]).

The obtained result is shown in Figure 2.1. The angles between the X-arm cavity axis and the local sensor's longitudinal axis of the ITMX-IP and ETMX-IP are obtained as 8.2 deg and 5.0 deg respectively.

This implies that the ITMX-IP motion and ETMX-IP motion in L DoF couples to the motion in the orthogonal axis of X-arm cavity axis by 1% and 0.4% respectively. It is confirmed that the ETMX and ITMX suspension are aligned to the X-arm cavity axis enough for the FPMI measurement[2].

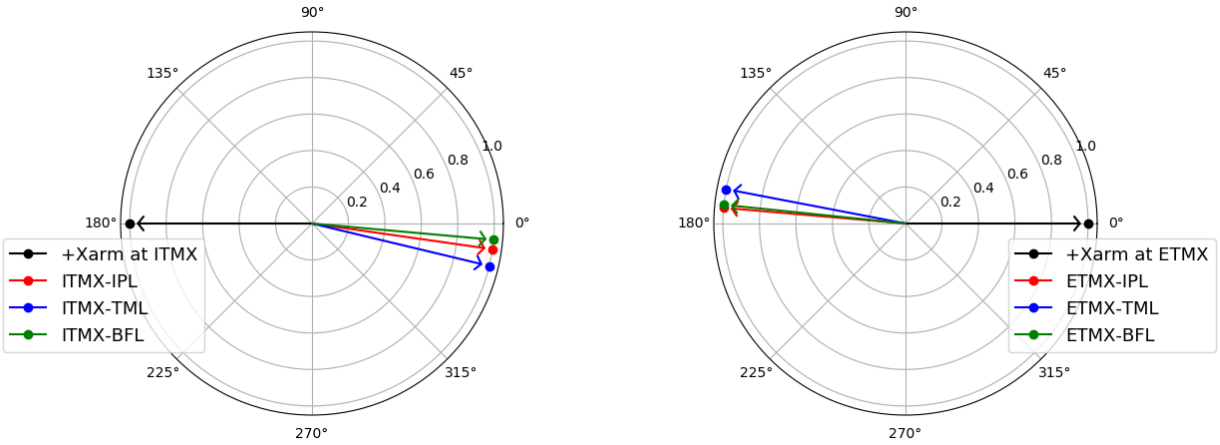

Figure 2.1: Measured angle difference of the ITMX suspensions ($left$) and ETMX suspensions ($right$) compared to the X-arm cavity axis.

[2] *What is the requirement for this?*

2.2 X-arm cavity length change with sensor correction

This subsection describes IP_{sc} performance more in detail. The target is to check if the IP_{sc} suppresses the X-arm cavity length change as expected.

For this purpose we use the X-arm cavity, which uses ITMX and ETMX. Both mirrors are suspended by the Type-A suspensions. We select the X-arm cavity since the local sensor at the TM-stage (the length-oplev) is too noisy to measure the TM motion without any actuation.

We use X-arm cavity for the simplicity, instead of the FPMI configuration.

As described in section 1.3, we implement the control filters to the ETMX suspension. Then we implement the filters to the ITMX suspension by mimicking the filters used for the ETMX suspension. We then measure the X-arm cavity length change with and without the IP_{sc}.

During this measurement, we consider that the implemented sensor correction system at the IP-stage (IP_{sc}) for both the ETMX and ITMX suspension works as designed.

In this measurement, the X-arm cavity is locked with IR laser and the displacement signal is reconstructed from its control signal (see section 5.1 in [1]).

2.2.1 Result with X-arm cavity length change

We describe the measured X-arm cavity displacement spectrum with and without the IP_{sc} for both ETMX and ITMX suspensions.

The result is shown in Figure 2.2. This figure shows the spectra X-arm cavity length change signal and the differential ground motion when the IP_{sc} for both the ETMX and ITMX suspensions is off. It also includes the coherence between these signals. In these plots, the differential ground motion is calculated from the two seismometers at EX and IX station in time domain.

This result shows the following facts:

1. The RMS of the X-arm cavity length change is suppressed by a factor of 2, for the integration down to 40 mHz.

2. At frequencies between 0.1 Hz to 0.6 Hz, the amplitude of the X-arm length change is reduced with the IP_{sc}. This is also shown in the coherence plot.

3. Below 0.1 Hz, the X-arm cavity length change is enhanced along with the seismometer noise floor, when the IP_{sc} is engaged. Especially with the IP_{sc}, the amplitude of the X-arm cavity length change is enhanced below 70 mHz. It is measured that this occurs due to the coupling from the seismometer for ITMX suspension, as shown in Figure 2.3 (see the black and the grey curves in the figure).

Consequently, the IP_{sc} for both ETMX and ITMX suspensions reduces the seismic noise coupling at frequencies between 0.1 Hz and 0.6 Hz, at the expense of the amplitude enhancement below 0.1 Hz. The measurement is qualitatively along with the expectation.

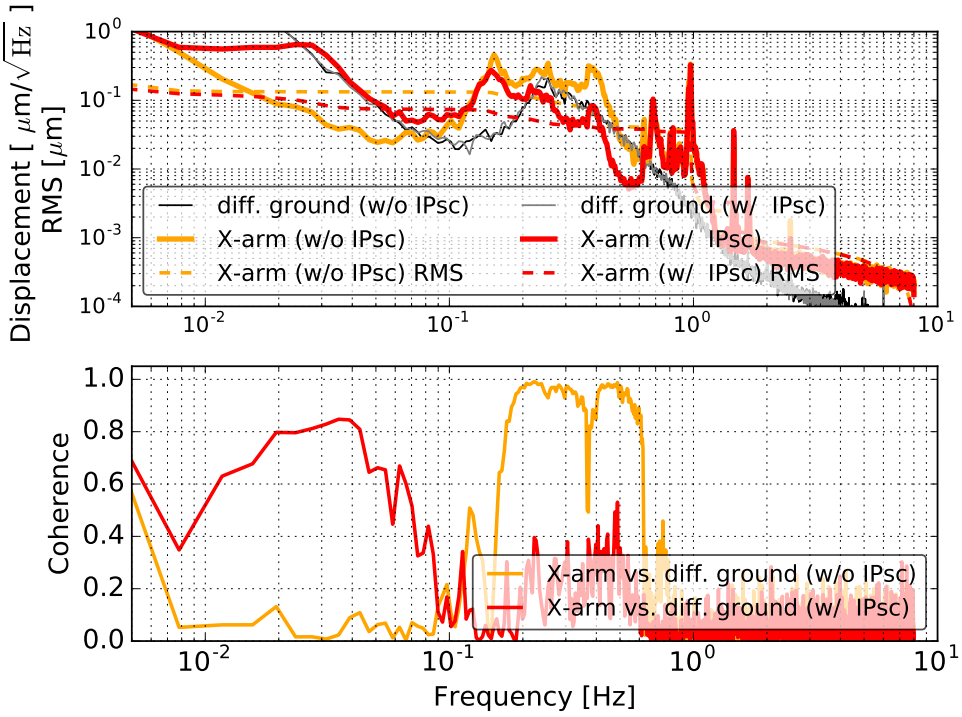

Figure 2.2: Comparison of the X-arm cavity length change with (red) and without (orange) the IP_{sc} for both ETMX and ITMX suspensions. The dashed curves draw the RMS values integrated down to about 50 mHz.

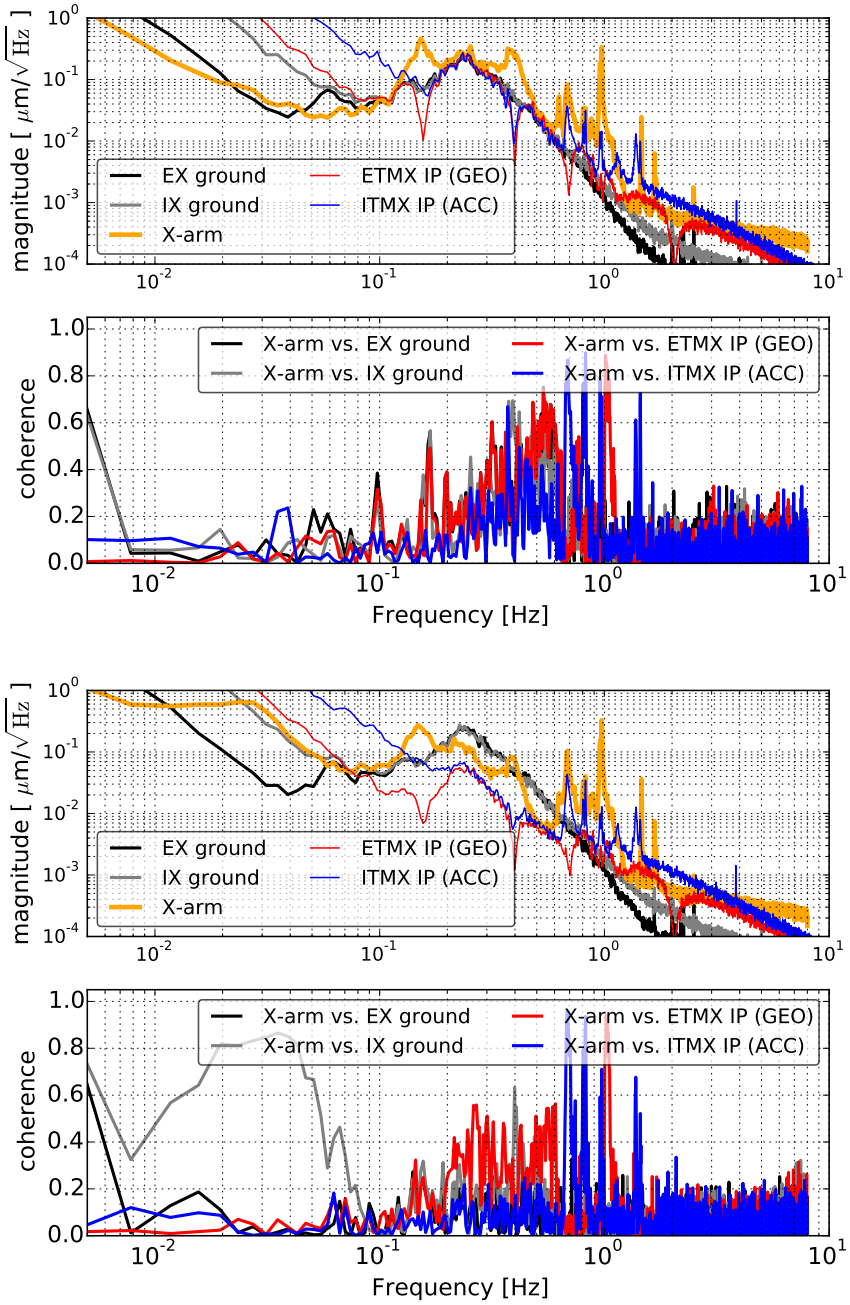

Figure 2.3: Measured spectra of the ground motion and the IP-stage motion measured by each local sensor, compared to the X-arm cavity length change. Without and with the IP_{sc} for both ETMX and ITMX suspensions are shown in *top* and *bottom* panel respectively. The orange curve are the same one shown in Figure 2.2. The black and grey colored curves show the local ground motion measured by the seismometers at EX- and IX-station respectively. The red and blue colored curves show the IP-stage motion measured by the geophones (GEO) and the TAMA accelerometers (ACC) respectively.

2.2.2 Estimation using single suspension measurement

Here we estimate the differential mirror displacement from the ground motion. If the transfer functions from the ground displacement to the mirror displacement of ETMX and the ITMX is described by $H_{\rm EX}$ and $H_{\rm EX}$ respectively, the X-arm cavity length change $x_{\rm Xarm}$ can be obtained by:

$$x_{\rm Xarm} \;=\; H_{\rm EX}\; x^{\rm EX}_{\rm GND} \;-\; H_{\rm IX}\; x^{\rm IX}_{\rm GND}, \tag{2.2}$$

where $x^{\rm EX}_{\rm GND}$ and $x^{\rm IX}_{\rm GND}$ are the ground motion at EX (X-end) and IX (X-front) station. For simplicity if we assume that both the suspensions has same response, i.e, $H_{\rm EX} = H_{\rm IX} \equiv H$, eq (2.2) can be written as:

$$x_{\rm Xarm} \;=\; H\;(x^{\rm EX}_{\rm GND} \;-\; x^{\rm IX}_{\rm GND}). \tag{2.3}$$

By using this assumption, the differential mirror displacement with and without the $\rm IP_{sc}$ for both ETMX and ITMX suspensions is shown in Figure 2.4. For this calculation, we use the measured H obtained using ETMX suspension (see section 7.4 in [2]).

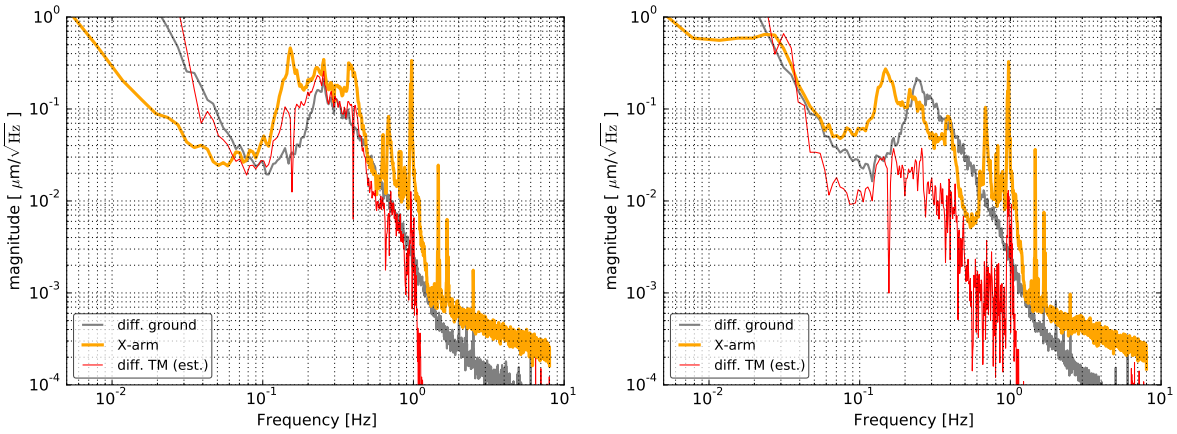

Figure 2.4: Estimated differential mirror displacement (red) compared to the measured X-arm cavity length change (orange). Without and with the $\rm IP_{sc}$ for both ETMX and ITMX suspensions are shown in *left* and *right* panel respectively. The grey colored curve shows the differential ground motion obtained from the seismometers at EX- and IX-station.

In the case *without* the $\rm IP_{sc}$, the estimated spectrum is along with the measured spectrum of the X-arm cavity length change in the frequency band between 70 mHz and 600 mHz, except for frequencies around 150 mHz and 400 mHz. Thus the assumption $H_{\rm EX} = H_{\rm IX}$ can be valid at frequencies between 70 mHz to 600 mHz. The measurement also agrees with the expectation except for these peaks.

The possible reason if the discrepancy at around 150 mHz and 400 mHz, the ETMX- and ITMX-suspension dose not have the same response ($H_{\rm EX} \neq H_{\rm IX}$). As another reason, coupling from the other DoFs than L DoF can also affect.

It is also observed that below 70 mHz, the X-arm cavity length change do not follow the differential ground motion measured by the seismometers. This is possibly caused by the tilt-coupling of the seismometers.

On the other hand, in the case *with* the IP_{sc}, it is found that the estimated spectrum has smaller amplitude especially above 40 mHz, compared to the amplitude of the X-arm cavity length change. Especially at 150 mHz, the estimation is smaller than the measurement by a factor of 8.

This measurement implies that, when the IP_{sc} is engaged, the noise coupling from the other DoFs than L DoF possibly becomes dominant especially above 40 mHz.

Generally speaking, more detailed investigation is necessary for the further RMS suppression of the X-arm cavity length change with the IP_{sc}. However, the further RMS suppression suppression can be achieved by:

1. building more identical mechanical responses and control filters between the ETMX and ITMX suspension so that the suspension frequency response of each suspension is same,

2. cutting the noise coupling form the other DoFs than L DoF[3],

3. damping the residual peaks at 150 mHz (and at 400 mHz).

2.2.3 Residual peak damping

Concerning the further RMS suppression, damping the residual peaks at 150 mHz will work. This residual peak gives the main contribution to the RMS displacement of the X-arm cavity length change in this measurement.

However, it is observed that the IPsc affects less the peak observed at about 150 mHz. This is so since we cannot control the IP-stage at the frequency due to its mechanical response. Figure 2.5 shows an example. It has a steep dip at 150 mHz, and it is difficult to set the open loop gain larger than 1.

[3]The detailed couplings are summarized in [1]. *The corresponding plots have to be generated for this measurement. Not yet done by May 5, 2020.*

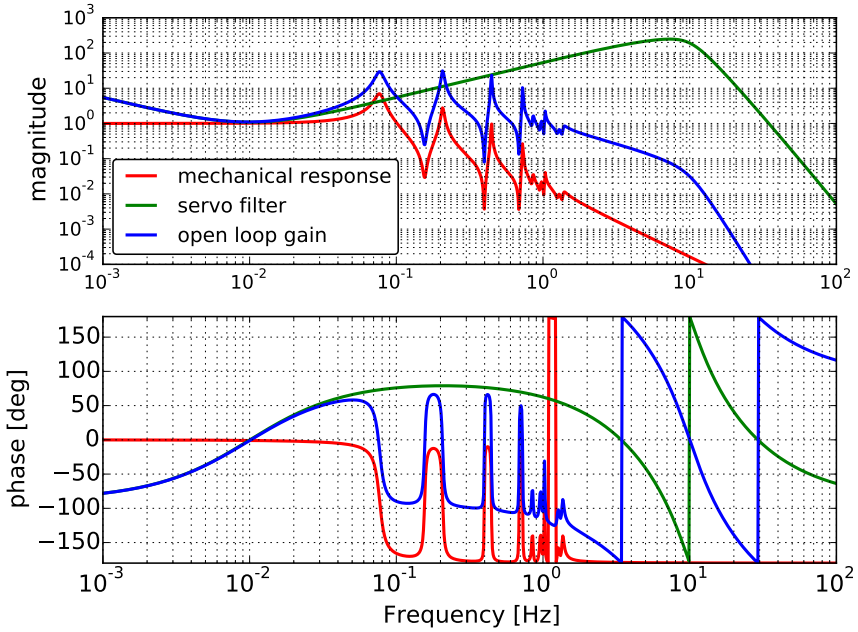

Figure 2.5: One of the designed control filters in the simulation. This is the case of IP-stage in L DoF. The red, green and blue colored curves represent the mechanical response (from the actuator to the IP sensor in displacement), the servo filter and the open loop gain respectively.

In order to suppress such peaks more, we need to engage other damping loops which senses either BF- or TM-stage motion.

Figure 2.6 and 2.7 show the transfer functions excited at the IP-stage and the BF-stage respectively. These are the transfer functions when the control loop is engaged at the IP-stage. This measurement is done using the ETMX suspension.

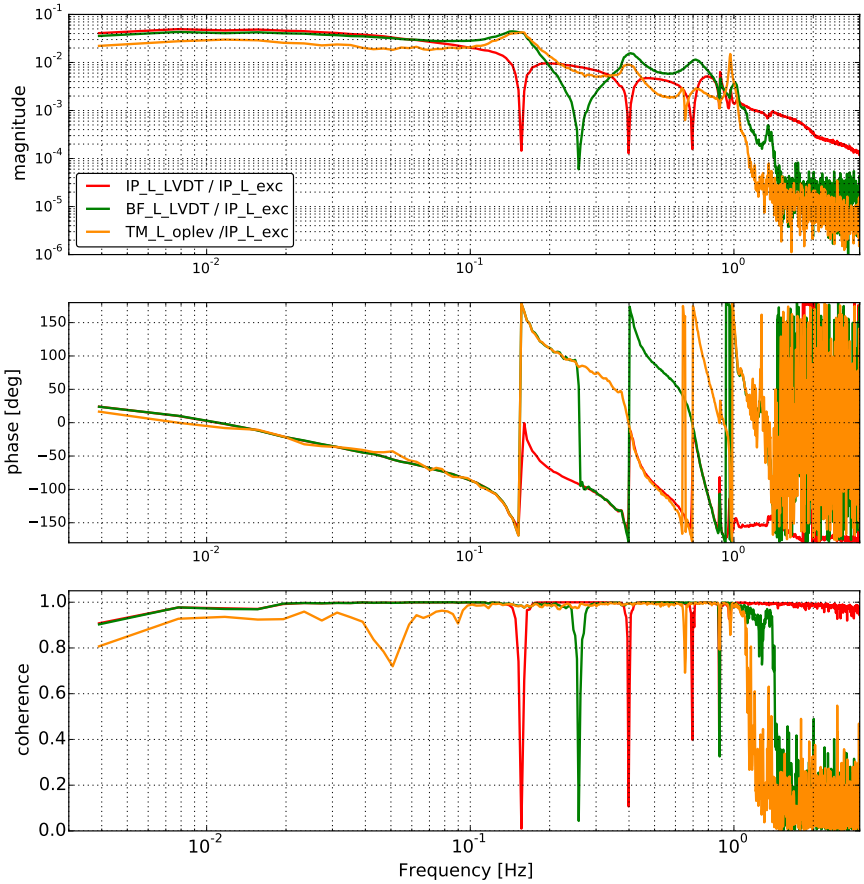

Figure 2.6: Force transfer function excited at the IP-stage with the IP-stage control. The used control loop is shown in Figure 2.5.

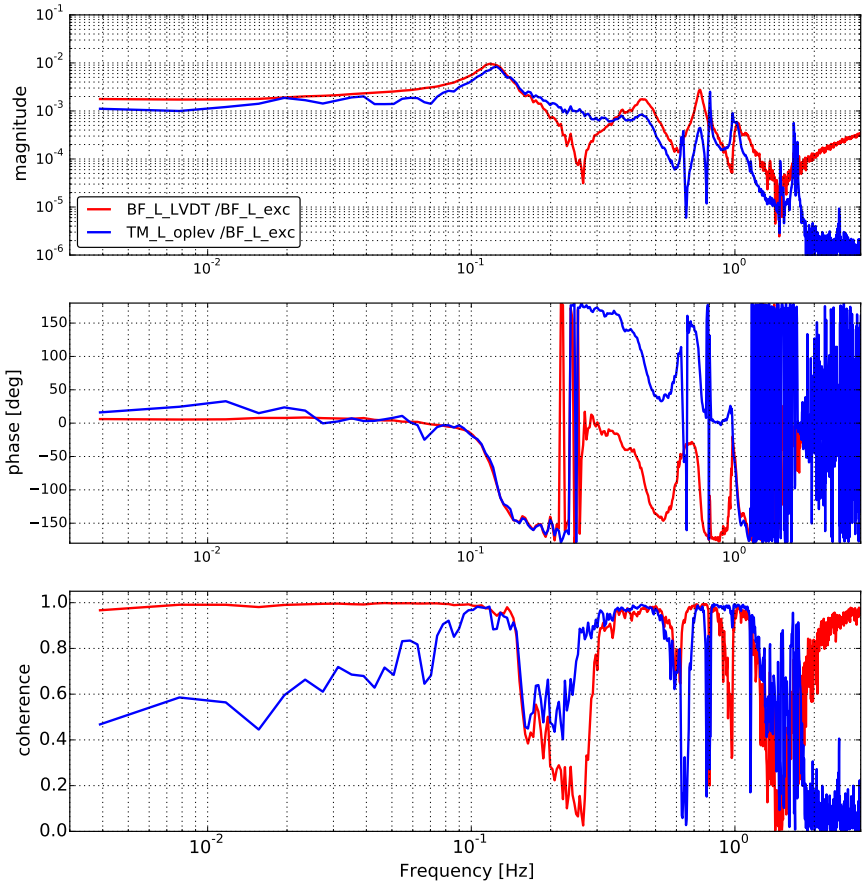

Figure 2.7: Force transfer function excited at the BF-stage with the IP-stage control. The used control loop is mostly same as shown in Figure 2.5. (The open loop gain looks a bit different from it. The dir of the corresponding measurement should be in either /users/VIS/ or /users/VISsvn/..)

We can damp the residual peaks at 150 mHz (and 400 mHz) by using BF-LVDTs. However, it is expected we will have a few difficulties:

1. If we want to use BF-LVDTs for the sensor, we have to use the sensor correction system also at this stage. Thus we will enhance the BF-body motion below 0.1 Hz due to the seismometer noise coupling.

2. The transfer function of the BF-stage has a steep dip at 250 mHz. Thus it might be difficult to set the open loop gain sufficiently large.

Then, the BF-LVDT damping (with the sensor correction) might help the easier lock acquisition, however, sometimes might not.

As another option, we can also damp the residual peaks (at 150 mHz) and 400 mHz by using the length-oplev at the TM-stage. However, the current TM length oplev is not sensitive enough to measure the TM motion, especially when the IP_{sc} is on. Also, even if the noise level becomes low enough, it is expewcted that we have to use the sensor correction at this TM-stage as well. We then have to treat the tilt-coupling of the seismometers below 0.1 Hz again.

Consequently, if we want to use the TM-stage for further suppression of the X-arm cavity length change, we will need to have both:

1. seismoemters which have good sensitivity below 0.1 Hz,

2. length optical levers which have better sensitivity.

2.3 Summary

Consequently, it is measured that:

1. the IP_{sc} at both ETMX and ITMX reduces the RMS displacement of the X-arm cavity length change (down to 40 mHz) by a factor of 2,

2. when the IP_{sc} is not engaged, the seismic noise coupling in L DoF can explain the X-arm cavity length change, except for the frequencies around 150 mHz and 400 mHz,

3. when the IP_{sc} is engaged, the seismic noise coupling in L DoF cannot explain the X-arm cavity length change. It seems that the other DoFs than L DoF affect the the X-arm cavity length change. It seems also due to the fact that the frequency responses of the ETMX and ITMX suspension are not identical.

For the further suppression of the X-arm cavity length change *with the sensor correction system*, it would be necessary to cut the noise coupling from the IX seismometer and also from the other DoFs. Even though we need to conduct further detailed measurement.

2.4 Future work

It is expected that we are going to use the inertial damping using the usual blending technique in the next observation run. Thus it is not clear that the 150 mHz or 400 mHz peaks, which cannot be damped with the IP-stage, become dominant in such system (maybe yes though).

However, it might be worth to consider a case where we close the damping loops using the BF-LVDTs or TM-length-oplev in such system. For that case, we need a system to cut the tilt-coupling of the seismometers below 0.1 Hz. To improve the sensitivity of the length optical lever would be also helpful.

Chapter A

Detailed characteristics of Type-A suspension

A.1 Type-A suspension configuration during the measurement

During the measurement period, we had to faced on a situation where at least on GAS filter is mechanically stack or locked in all the Type-A suspensions. Concerning ETMY suspension, we found that second and third GAS stages seemed to be mechanically stack with same reason as the issue of ETMX F2-GAS filter. For the two input suspensions, we had to intentionally lock the first GAS filter (called F0-GAS) keystone in order to hold the other suspension components, especially the mirror, at the target height[1]. For all these suspensions we decided to keep using them with such configuration for the O3 period. Figure A.1 shows the expected mechanical seismic attenuation performance where one or two GAS stage are not working as spring, assuming the vertical mirror vibration couples to the longitudinal DoF by 1%.

[1]This issue has the following history: we originally had GAS blades made in abroad which would suspend the mirror properly. We then found that the original blade was actually broken, cracked because of hydrogen embrittlement in Maraging steels [3]. We remade and replaced the blades with the new ones made in Japan, we finally found that the newly made GAS blades were too weak to hold the whole suspension at the desired height.

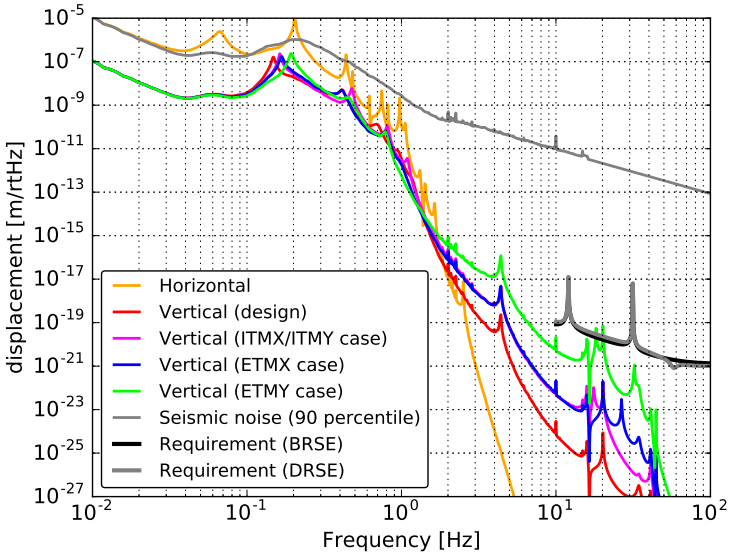

Figure A.1: Expected mechanical seismic attenuation performance where one or two GAS stage are not working as spring, assuming the vertical mirror vibration couples to the longitudinal DoF by 1%.

A.2 Typical noise floors of inertial sensors

The typical noise floors of the inertial sensors used for current Type-A SAS, compared to the mirror displacement due to the seismic noise, are summarized in Figure A.2. This plot includes the spectra of the displacement of the mirror suspended by the Type-A SAS where the seismic noise level is high/low.

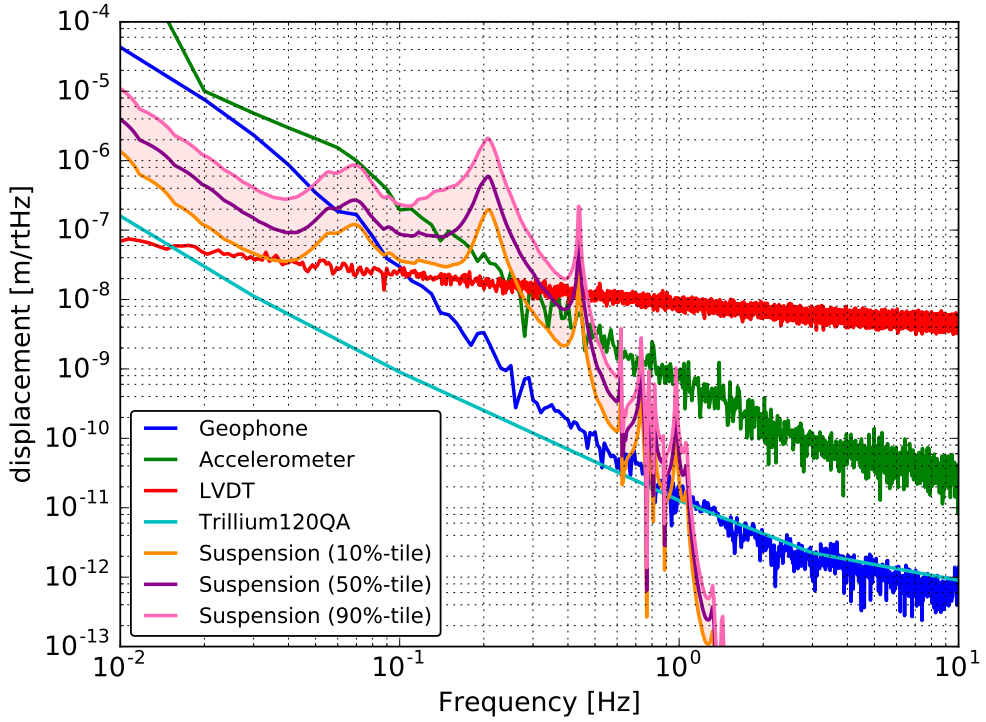

Figure A.2: The typical noise floors of such inertial sensors compared to the mirror displacement due to the seismic noise.

Bibliography

[1] K. Miyo. PhD Thesis, University of Tokyo. 2020.

[2] Y. Fujii. PhD Thesis (in prep. May 5, 2020), University of Tokyo. 2020.

[3] M. Barsanti, M. Beghini, F. Frasconi, R. Ishak, B.D. Monelli, and R. Valentini. Experimental study of hydrogen embrittlement in maraging steels. *Procedia Structural Integrity*, 8:501 – 508, 2018. AIAS2017 - 46th Conference on Stress Analysis and Mechanical Engineering Design, 6-9 September 2017, Pisa, Italy.